

## ASSESSMENT OF THE DURATION OF TIME REQUIRED FOR CONVENTIONAL Ti-Ni SINTERING

N. ZHANG\*, P. BABAYAN KHOSROVABADI, J.H. LINDENHOVIUS and B.H. KOLSTER

*Foundation for Advanced Metals Science, Enschede, The Netherlands**\*S.G.M. P.O. Box 8039, 7550 KA, Hengelo (O), The Netherlands*

**ABSTRACT** Elemental blends of Ti-Ni powder in the Ti50Ni50 ratio were tested by the conventional press and sintered method. The sintering conditions employed were based on solid-state diffusion which resulted in a homogeneous alloy exhibiting the shape-memory effect. An attempt has been made to establish a mathematical model to predict the time required for complete homogenization. The comparison of the calculated values with that of the experimental results revealed consistency.

## 1.-INTRODUCTION

Powder metallurgy is an alternative method of manufacturing products which is receiving an ever increasing attention with obvious economic benefits. The importance of this approach lies in the possibility of producing novel materials (such as TiNi), in which conventional techniques are cumbersome. Sintering of the elemental blend of Ti-Ni powder is an alloying process with the aim to achieve intermetallic compounds of TiNi [1-6]. However the concept of sintering of these powders is rather complicated and is dependent upon the set conditions. If the sintering process is carried out beneath 940°C (which is the lowest eutectic point, see fig.1), and with a moderate heating rate, the process will be controlled by solid-state diffusion, otherwise a reactive combustion may prevail [8]. It is the aim of this paper to concentrate and study the solid-state diffusion process in this alloy, and attempt is made to predict the homogenization process by employing a mathematical model.

## 2.-EXPERIMENTAL

Pure Ti and Ni powders having purities of 99.5% and 99.9% respectively with a particle size of  $\sim 45 \mu\text{m}$  were employed in this study. The powders were blended in a cylindrical mixer and compacted in an uniaxial mode. The relative green densities of the compacts were 80% of the theoretical value. The compacts prepared had a mean alloy composition of Ti50Ni50 (at%). Sintering was conducted under Argon atmosphere, by first pre-vacuuming to  $10^{-5}$  Torr, heating up period till the final set temperature was selected as: first heating up to 600°C by 20°C/min, then 10°C/min to 700°C followed by 2°C/min in the range of 750-900°C. The reason for the low heating rate at the last stage is to prevent combustion. All sintered samples were subjected to SEM and X-ray micro-analysis. To detect the transformation characteristics of the samples,

a DSC (differential scanning calorimeter) was employed in order to determine  $M_s$ ,  $M_f$ ,  $A_s$ ,  $A_f$  and the latent heats. Finally, samples were subjected to mechanical testing, observing their SME (shape-memory effect).

3.-PHENOMENOLOGICAL APPROACH ON THE Ti-Ni SOLID STATE DIFFUSION

Mass transport during sintering of Ti-Ni powders will occur, by mutual fluxes of Ti and Ni atoms diffusing oppositely within the distance of two neighbouring particles of different elements, as shown schematically in Fig.2 a. Figs.2 b-e represent the distribution of Ni molar concentration along the direction of aligning centers of the two connected Ti and Ni particles, as the time progresses.

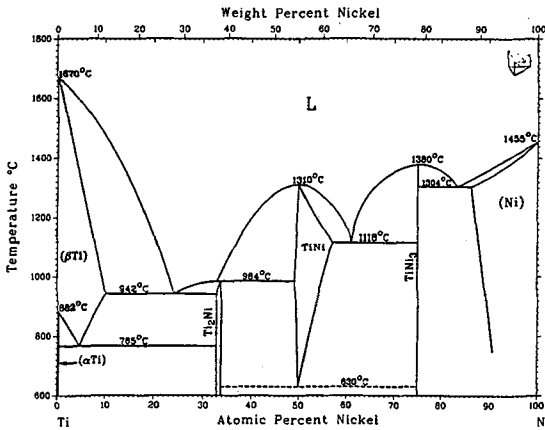


Fig.1 The Ti-Ni binary phase diagram [7]

To predict the homogenization process we refer to Fig.2, in which point o is the position of the original interface between the Ti and Ni particle. This reference point is considered to be fixed and does not change with the progressive change of the structure, which is obviously an approximation.  $x$  is the distance from the Ti-rich side of the TiNi layer to point o and  $y$  the distance from the Ni-rich side to point o. During sintering, when the TiNi layer grows into its neighbouring Ti<sub>2</sub>Ni layer by a step  $\Delta x$  in time  $\Delta t$ , the Ti<sub>2</sub>Ni layer contracts by a step  $\Delta x'$ ; then the concentration will change from  $C_1$  to  $C_2$ , where  $C_1$  is Ni moles per unit Ti<sub>2</sub>Ni volume and  $C_2$  the same per unit TiNi volume at the Ti-rich side

(close to Ti<sub>2</sub>Ni) of the TiNi layer. It is assumed to be caused by Ni mass flux,  $J$ , flowing to the interface of TiNi/Ti<sub>2</sub>Ni; thus, we can express

$$C_2\Delta x - C_1\Delta x' = C_2\Delta x - C_1k_1\Delta x \approx J \cdot \Delta t \tag{1}$$

where  $k_1 = \Delta x' / \Delta x$  is a conversion coefficient due to the different molar volumes of Ti<sub>2</sub>Ni and TiNi. Basing on Fick's first law, Eq.(1) turns into

$$\Delta x \cdot (C_2 - k_1 C_1) \approx -\bar{D} \cdot \frac{\partial C}{\partial x} \cdot \Delta t$$

or 
$$(C_2 - k_1 C_1) \cdot dx = -\bar{D} \cdot \frac{\partial C}{\partial x} \cdot dt \tag{2}$$

where  $\bar{D}$  is the chemical diffusion coefficient for the TiNi phase and  $\frac{\partial C}{\partial x}$  the concentration gradient in this phase (it should be stressed that  $\frac{\partial C}{\partial x}$  is the gradient at the point of boundary of TiNi with Ti<sub>2</sub>Ni).

The concentration gradient in the TiNi layer has been assumed to be linear, even though this is not an accurate assumption. However, the observed experimental results have indicated linearity [9]. Thus we have

$$\frac{\partial C}{\partial x} = \frac{C_2 - C_3}{x+y} \tag{3}$$

In order to conserve the mass balance ratio,  $y$  and  $x$  must be correlated, e.g., in the case of Fig.3-1 d, Ni moles in  $Ti_2Ni$  plus those in  $TiNi_3$  should be equal to the sum of the Ti moles in both phases, which leads to

$$(k_2R - k_1x)C_1 + (k_4R' - k_3y)C_4 = (k_2R - k_1x)C_1 + (k_4R' - k_3y)C_4 \quad (4)$$

where,  $R$  and  $R'$  are radii of the Ti and Ni particles;  $C_4$ ,  $C_1$  and  $C_4'$  are concentrations of Ni in the  $TiNi_3$  phase, Ti in the  $Ti_2Ni$  phase and Ti in  $TiNi_3$  in moles per unit volume;  $k_2$ ,  $k_3$  and  $k_4$  are molar-volume ratios of  $Ti_2Ni$  to Ti,  $TiNi_3$  to  $TiNi$  and  $TiNi_3$  to Ni, respectively. If the number of atoms in one Ti particle is equal to that in one Ni particle we can relate  $R'$  with  $R$  by  $R' = k_5R$ , where  $k_5$  is a conversion ratio of dimensions. Combining Eq. (3), Eq. (4) and  $R' = k_5R$  with Eq. (2) leads to a differential equation

$$dt = \frac{C_2 - k_1C_1}{k_3\bar{D}(C_3 - C_2)} \left[ \left( k_3 + k_1 \frac{C_1 - C_1'}{C_4 - C_4'} \right) x + \left( k_4k_5 - k_2 \frac{C_1 - C_1'}{C_4 - C_4'} \right) R \right] dx \quad (5)$$

The fulfillment of homogenization could be judged by the fact that the  $TiNi$  layer reaches the center of the original Ti particle, i.e.,  $x = k_2R/k_1$  in Fig.2 e. Integrating Eq. (5) from 0 to  $k_2R/k_1$  with respect to  $x$ , we can obtain the time required for complete homogenization

$$t_f = \frac{k_2(C_2 - k_1C_1)}{k_1(C_3 - C_2)} \left( \frac{k_2}{2k_1} + \frac{k_4k_5}{k_3} - \frac{k_2(C_1 - C_1')}{2k_3(C_4 - C_4')} \right) \frac{R^2}{\bar{D}} \quad (6)$$

It is important to emphasize that the consideration with respect to Eq.(1) constitutes only the in-flux of Ni ( $J$ ), while the out-flux of Ni ( $J'$ ) which also flows from the transformed region into the  $Ti_2Ni$  layer has been neglected. Otherwise the right hand side of Eq.(1) would have taken the following form of  $(J - J')\Delta t$ . However, due to the narrow

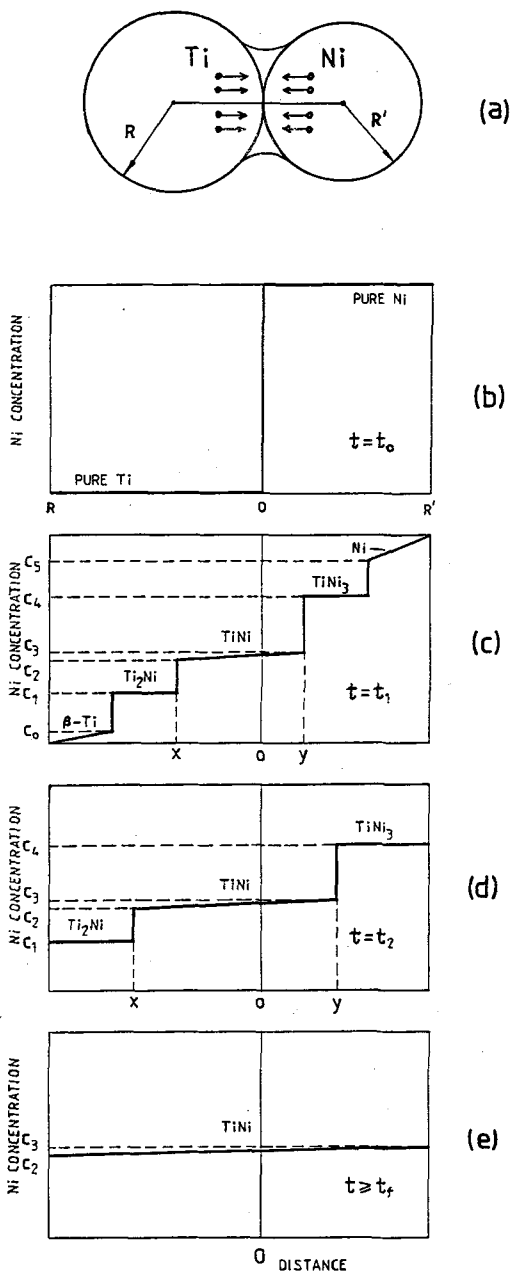


Fig.2 Schematic profiles of the solid-state Ti-Ni diffusion in one dimension  
 a) Connection of a Ti particle with a Ni one  
 b-e) Ni molar concentration distribution along the align of the centers of the two particles

homogeneity range of the Ti<sub>2</sub>Ni phase and the lack of available data of diffusion in this phase [10], omission of J' is inevitable. On the other hand, such an omission is acceptable if one notices the fact that

- 1) J' will always be less than J,
- 2) the existing composition range of the Ti<sub>2</sub>Ni phase is rather narrow. Especially after the β-Ti phase vanishes during sintering, see Fig.2d,
  - a) either, the chemical potential difference (responsible for J') inside Ti<sub>2</sub>Ni is small, corresponding to the small composition difference, thus, J' is negligible;
  - b) or, if the chemical potential difference is not small and if J' is substantial, the Ti<sub>2</sub>Ni layer will be saturated immediately due to J', viz, will reach the composition in equilibrium with the TiNi phase. Consequently, the further diffusion should stop completely, J'=0.

Therefore, it is reasonable to assume the present form of Eq.(1) for the purpose of approximating the time required for homogenization.

#### 4.-EXPERIMENTAL RESULTS

##### 4.1.-Structure Analyses

Sintering was conducted at 900°C. The molar concentrations at this temperature were determined, by considering the lattice parameters, and their corresponding atomic compositions based on the Ti-Ni binary phase diagram. The results are presented below:

$$\begin{array}{lll} C_1=3.663 \times 10^{-2}, & C_2=6.004 \times 10^{-2}, & C_3=6.540 \times 10^{-2}, \\ C_4=10.598 \times 10^{-2}, & C_1=7.326 \times 10^{-2}, & C_4=3.533 \times 10^{-2}, \end{array}$$

in units of mol/cm<sup>3</sup>, and

$$k_1=1.1082, \quad k_2=0.8557, \quad k_3=0.8618, \quad k_4=1.0743, \quad k_5=0.8525$$

The chemical diffusion coefficient in the TiNi phase with 50 at% Ni at 900°C was taken as  $\bar{D}=9.5 \times 10^{-10}$  cm<sup>2</sup>/sec, according to Lit.[10]. The particle size of the Ti and Ni powders is 45 μm (R=45/2μm). By substituting all the above values in Eq.(6), it is now possible to predict the time for total homogenization, which yields  $t_f=4.9$  hr.

Fig.3 a-d reveal the progressive change in microstructure of the samples sintered at 900°C. As it can be noticed Fig.3 a represents the starting point where the pure Ti and Ni particles are in contact with each other, this clearly corresponds to Fig.2 b. As the process continues, after an hour (Fig.3 b), the microstructure is revealing formation of intermediate phases, the dark region representing β-Ti and bright clusters being Ni (plus TiNi<sub>3</sub>), light grey corresponding to TiNi and dark grey representing Ti<sub>2</sub>Ni, which relates to Fig.2 c. Fig.3 c represents the microstructure after 3 hours of holding time. As it can be noticed only three phases are present, corresponding to the TiNi matrix, Ti<sub>2</sub>Ni grey area and TiNi<sub>3</sub> light grey area, respectively. Such a structure correlates to Fig.2 d. Finally, Fig.3 d represents the sample after 5 hours of holding time indicating almost a single phase with slight relics of TiNi<sub>3</sub> phase. The presence of the second phase is probably due to the non-uniform distribution of the powders during the blending process. Nonetheless the experimental results are in good agreement with that of the predicted values, and justify the application of the model discussed in section 3.

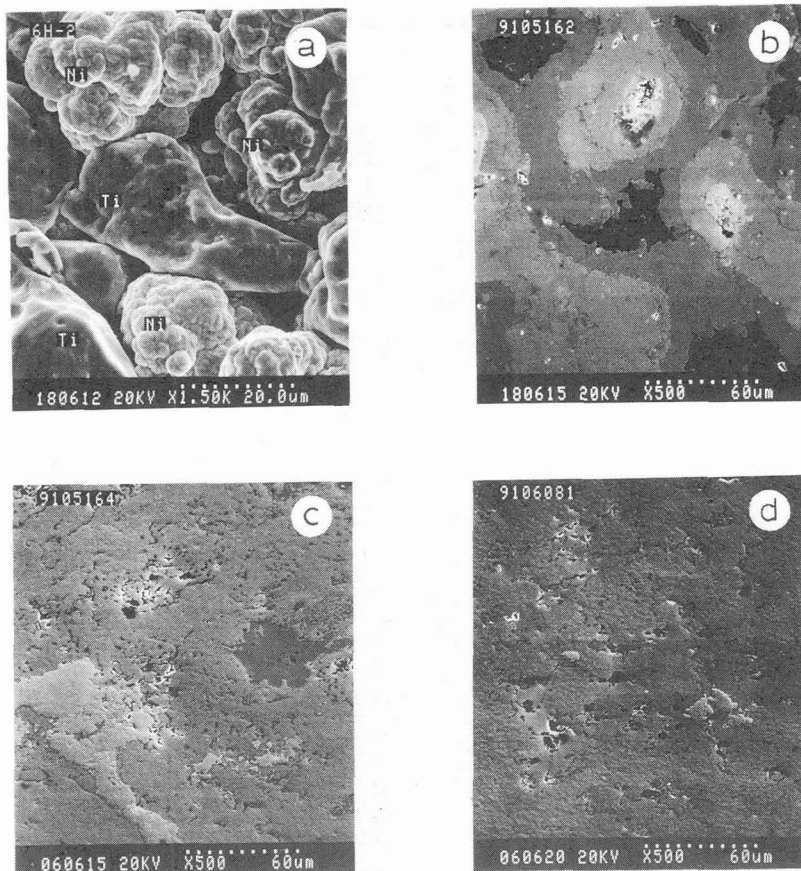


Fig.3 Microstructures of the Ti50Ni50 samples observed by SEM  
 a) A cross-section of a compact before sintering  
 b-d) sintered at 900°C for 1hr, 3hr and 5hr respectively

#### 4.2.-SME of the Sintered TiNi Alloy

The results of the DSC measurement on the samples sintered for 5 hours at 900°C, revealed the following values:  $M_s=68^\circ\text{C}$ ,  $M_f=-14^\circ\text{C}$ ,  $A_s=44^\circ\text{C}$  and  $A_f=110^\circ\text{C}$  (with  $\Delta H=24\text{ mJ/mg}$ ). Fig.4 represents such a curve. It is notable that the thermal peak of the martensitic transformation from  $M_s$  to  $M_f$  is much broader than the peak obtained for the cast alloy, and the reverse transformation exhibits dual peaks, which implies the presence of a transition. The reason for such discrepancies are related to the composition difference existing within the individual grains.

In addition, the same sample sintered at 900°C for 5 hours was subjected to tensile testing (Fig.5) by applying a load ( $\sigma_a$ ) in the martensitic state, and then unloading the sample, where it exhibits a plastic strain of  $\epsilon_b$ . Keeping the sample fixed in position (within the clamps) and heating the whole sample above the  $A_f$  temperature, a spontaneous stress  $\sigma_c$  was recorded due to SME. Finally it was unloaded and the strain of it was corresponding to the new

value of  $\epsilon\alpha$  (see Fig.5). It is important to emphasize that the data presented are subject to several repeated tests (mechanical training) to achieve a stable SME. From the above results it is found that the recovery force corresponds to  $\sigma_c=195$  MPa and the degree of the recovery,  $\gamma=(\epsilon_b-\epsilon_d)/\epsilon_b$ , approximates to 67%. Furthermore, the non linearity of curve *ab* of Fig.5 is due to the stress-induced martensitic transformation. Finally, 67% (not full) recovery is apparently due to existence of porosity in the sintered sample.

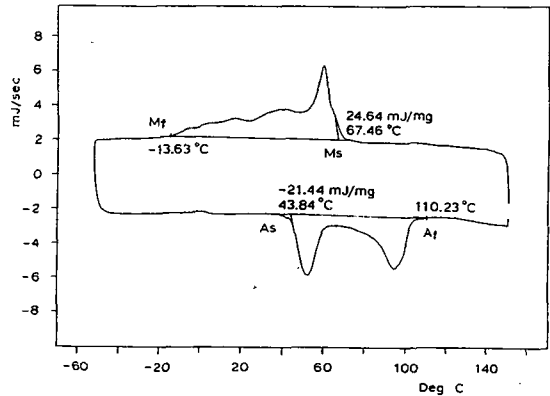


Fig.4 Thermal-analysis curve of the TisoNiso alloy sintered at 900 °C for 5hr

## 5.-CONCLUSIONS

-Duration of time ( $t_f$ ) for complete homogenization of Ti-Ni (having equal particle size) is parabolic with respect to the powder size, i.e,  $t_f=k \cdot R^2$ , where  $k$  is a proportionality factor.

-According to calculated results based on the chemical diffusion coefficient of the TiNi compound, sintering of the 45  $\mu\text{m}$  elemental powders at 900 °C requires 5 hr to achieve a homogenized TiNi alloy.

-The experimental results indicate similar duration for complete homogenization. The prepared TiNi alloy exhibits the shape-memory effect.

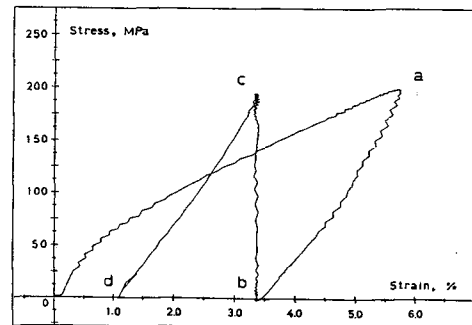


Fig.5 Stress-strain characteristics of the sintered TisoNiso alloy on SME tensile testing

## REFERENCES

- [1] G.I.Aksenov, I.A.Drozdov, A.M.Sorokin, D.B.Chernov and Yu.A.Atyakshev. *Sov.Powder Metall.Met.Ceram.*, Vol.20(1981), P.340.
- [2] K.Funami, Y.Sekiguchi and H.Funakubo, *J.Jap.Inst.Metals*, Vol.48, No.11(1984), P.1113.
- [3] M.Igharo and J.V.Wood, *Powder Metall.*, Vol.28, No.3(1985), P.131.
- [4] R.M.Andrews-Koryta and W.N.Weins, *Proc. 25th Annual Conf. Metallurgists*, (1986), P.283.
- [5] D.G.Morris and M.A.Morris, *Mat.Sci.Engin.*, A110(1989), P.139.
- [6] H.Kuroki, M.Nishio and C.Matsumoto, *J.Jpn.Soc.Powder Metall.*, Vol.36, No.6(1989), P.701.
- [7] "Binary Alloy Phase Diagrams", Vol.2, P.1768, ASM, Metals Park, Ohio44073.
- [8] H.C.Yi and J.J.Moore, *Scripta Metall.*, Vol.22, (1988), P.1889.
- [9] G.F.Bastin and G.D.Rieck, *Metall.Trans.*, Vol.5, (1974), P.1817.
- [10] G.F.Bastin and G.D.Rieck, *Metall.Trans.*, Vol.5, (1974), P.1828.